Holography for Heavy-Ion Collisions at LHC and NICA.

Results of the last two years

Irina Aref'eva[1,*]

[1]Steklov Mathematical Institute, Russian Academy of Sciences,
Gubkina str. 8, 119991, Moscow, Russia

Abstract. In the previous Quarks 2016 conference I have presented a concise review of description of quark-gluon plasma (QGP) formation in heavy-ion collisions (HIC) within the holographic approach. In particular, I have discussed how to get the total multiplicity and time formation of QGP in HIC that fit the recent experimental data. For this purpose we had to use an anisotropic holographic model. There are also experimental indications that QGP formed in HIC is anisotropic. In this talk I discuss static properties of anisotropic QGP, in particular, phase transition and diffusion coefficients.

1 Introduction

It is my pleasure to give a talk in the Quarks 2018 Conference. I would like to thank the organizers for the invitation. The subject of my talk is the same as in the previous Quarks 2016 Conference, it is about the holography description of quark-gluon plasma (QGP) formed in heavy-ion collisions (HIC) [1]. Last time I have discussed how to get the total multiplicity and time formation of QGP in HIC that fit the recent experimental data. The main point was the use of anisotropic 5-dim metric in holographic description. The anisotropy is a natural assumption due to geometry of HIC. There are experimental indications that QGP formed in HIC is anisotropic [4]. In this talk I mainly discuss static properties of anisotropic QGP formed in HIC. All details about physical picture of formation of QGP in HIC and gauge/gravity dual approach to physical problems related to QGP the reader can find in [1–3] and refs therein. Here I just would like to mention that I'll use the so-called the bottom-up holographic approach. In this approach we choose a 5-dim gravity to get phenomenologically acceptable theory on the 4-dimensional boundary.

2 Holographic setup

2.1 Dual model [5]

The gravitational theory dual to the anisotropic field theory considered in [5] is defined by the Einstein-Dilaton-two-Maxwell (Einstein-Dilaton-Maxwell-Maxwell) action with special potentials V for the dilaton field ϕ and potentials f_1 and f_2 for two Maxwell fields:

$$S = \frac{1}{16\pi G_5}\int d^5x\sqrt{-g}\left[R - \frac{1}{4}f_1(\phi)F^2_{(1)} - \frac{1}{4}f_2(\phi)F^2_{(2)} - \frac{1}{2}(\partial\phi)^2 - V(\phi)\right], \qquad (1)$$

*e-mail: arefeva@mi.ras.ru

where $F^2_{(1)}$ and $F^2_{(2)}$ are the squares of the Maxwell fields.

The ansatz with the Maxwell fields $F_{(1)\mu\nu} = \partial_\mu A_{(1)\nu} - \partial_\nu A_{(1)\mu}$, $A_{(1)\mu} = A_t(z)\delta^0_\mu$, and $F_{(2)} = q\, dy^1 \wedge dy^2$, $\phi = \phi(z)$ and metric

$$ds^2 = \frac{L^2 b(z)}{z^2}\left[-f(z)dt^2 + dx^2 + \left(\frac{z}{L}\right)^{2-\frac{2}{\nu}}\left(dy_1^2 + dy_2^2\right) + \frac{dz^2}{f(z)}\right], \quad b(z) = e^{P(z)}, \tag{2}$$

satisfies the equations of motion under relations between the warp factor $b(z)$, dilaton and Maxwell potential [5]. The ansatz (2) breaks isotropy while preserves translation and (t, x)-boost invariances. Here $f(z)$ is the blackening function and L is the characteristic length scale of the geometry and we set $L = 1$. The 5-dim Einstein-Dilaton-Maxwell-Maxwell theory can be considered as a truncated supergravity IIA similar to [7]. Note that the second Maxwell field in this case can occur due to compactification. Another possible underlying theory is the 5d SO(6) gauged supergravity [8].

$b(z) = \exp cz^2$-model. In [5] the anisotropic model with a quadratic exponent as b-factor has been considered. The advantage of this model is that in this case we can find potentials V, f_1 and f_2 and the blackening function f explicitly. It is amusing to note, that this choice corresponds to the dilaton potential that can be approximated by the sum of two exponents:

$$V(\phi, \mu, \nu) = V_0(\nu) - C_1(\mu, \nu)e^{k_1(\nu)\phi} + C_2(\mu, \nu)e^{k_2(\nu)\phi}. \tag{3}$$

The best fit is given by $V_0(4.5) = -0.5778$, $k_1(4.5) = 0.7897$, $k_2(4.5) = 2.0995$ with the coefficients depending on the chemical potential μ, Fig.1.A: $C_1(\mu, 4.5) = 23.0779 + 2.4236\mu^2$, $C_2(\mu, 4.5) = 0.0575 + 4.9919\mu^2$.

In isotropic case, Fig.1.B, the approximation constants are: $V_0(1) = -10.8689$, $k_1(1) = 1.0852$, $k_2(1) = 2.4103$, $C_1(\mu, 1) = 27.2825 + 4.3749\mu^2$, $C_2(\mu, 1) = 0.0031 + 5.03093\mu^2$.

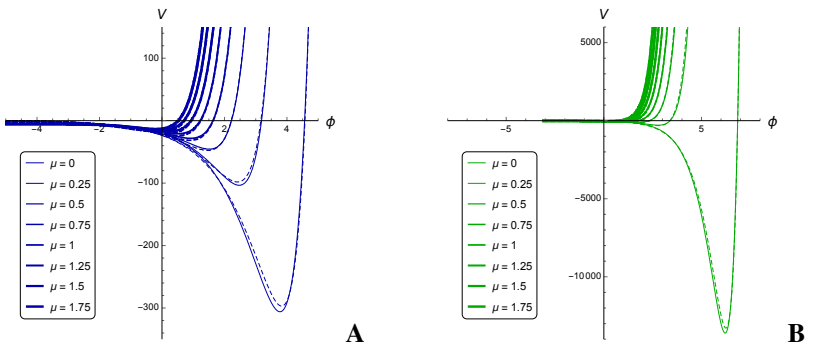

Figure 1: Scalar field potential $V(\phi)$ (solid lines) and its approximation (dashed lines) as a sum of two exponents and a constant $V_0(\nu)$ for $z_h = 1$, $c = -1$ and different μ in anisotropic, $\nu = 4.5$, (**A**), and isotropic, $\nu = 1$ (**B**), cases.

Note, that in [10] an explicit isotropic solution for the dilaton potential as a sum of two exponents and zero chemical potential has been constructed. It would be interesting to generalize this construction to the anisotropic and non-zero chemical potential cases.

UV asymptotics. The metric (2) near the boundary $z \to 0$ is asymptotically

$$ds^2 \sim \frac{L^2}{z^2}\left[-dt^2 + dx^2 + \left(\frac{z}{L}\right)^{2-\frac{2}{\nu}}\left(dy_1^2 + dy_2^2\right) + dz^2\right], \tag{4}$$

it is supported by

$$f_1(z) = z^{-2+\frac{2}{\nu}}, f_2(z) \sim \frac{c(\nu)}{z^{4/\nu}}, \quad \phi \sim \frac{2\sqrt{\nu-1}}{\nu} \log \frac{z}{z_h}, \tag{5}$$

$c(4.5) = 3.80$, $c(1) = 0$ [9]. To embed the 4-dim space-time to the metric (2) we can assume that we deal with the section $z = a$, where a is an arbitrary scale parameter. The corresponding 4-dim spacetime exhibits the scaling $t \to \lambda t$, $x \to \lambda x$, $\vec{y}_\perp \to \lambda \vec{y}_\perp^{1/\nu}$, $a \to \lambda a$, which we call $\mathcal{L}_{2,2}$-scaling. We assume that effectively such geometry takes into account the non-isotropic geometry of HIC and has as a holographic dual a gauge theory with $\mathcal{L}_{2,2}$ scaling, that can be understood as a continuous version of a lattice gauge theory on the anisotropic lattice [11].

We are interested in a deformation of the geometry with $\mathcal{L}_{2,2}$-scaling, that can describe confining gauge theories and that corresponds to a nontrivial warp factor. The case of $b(z) = e^{cz^2/2}$ admits the explicit solution [5] and is considered in this paper. More involved forms of the warp factor admit only numerical solutions (compare with [6]) and perhaps will be needed for a more realistic model.

Comparison with RT model. It is instructive to compare our anisotropic model (2) with other popular holographic anisotropic model based on the Mateos-Trancanelli metric

$$ds^2 = \frac{L^2 \mathfrak{b}(z)}{z^2}\left[-\mathfrak{g}(z)dt^2 + e^{2h(z)}dx^2 + d\vec{y}_\perp^2 + \frac{dz^2}{\mathfrak{g}(z)}\right] \tag{6}$$

This metric is supported by the Einstein-Axion-Dilaton action

$$S = \frac{1}{16\pi G_5}\int d^5x\sqrt{-g}\left[R - \frac{1}{2}Z(\phi)(\partial\chi)^2 - \frac{1}{2}(\partial\phi)^2 - V(\phi)\right], \tag{7}$$

Dilaton theory can be realized in terms of D3/D7 branes in IIB string theory when $V = 12$ and $Z = e^{2\phi}$ [13–15]. In this case the underlying field theory is conformal. When one is interested in a non-conformal solution, a more generic choice of the potentials V and Z [16–19] is suitable. For the quadratic dilaton potential the theory in the region $z \to \infty$ exhibits a Lifshitz-like scaling $t \to \lambda t$, $\vec{y}_\perp \to \lambda \vec{y}_\perp$, $z \to \lambda z$, $x \to \lambda^{\frac{1}{\xi}} x$. For more complicated dilaton potential the metric (6) has the hyperscaling violation property.

2.2 Born-Infield (BI) model for non-local observables

Wilson loops play important role in study of gauge theories, see for example [20]. In the context of AdS/CFT the spacial Wilson loops were discussed in [21]. For anisotropic case their have been studied in [22], but without the deformation factor $b(z)$. To consider different Wilson loops it is useful to consider a general BI action

$$\mathcal{S} = \frac{T}{2\pi\alpha}\int_{-\ell}^{\ell} M(z)\sqrt{F(z) + z'^2}dx, \tag{8}$$

$z' = \partial_x z$. The first integral has the form $\frac{M(z)F(z)}{\sqrt{F(z)+z'^2}} = \mathcal{J}$ and its value can be related with the "top" point z_*, i.e. $\mathcal{J} = \frac{M(z_*)F(z_*)}{\sqrt{F(z_*)}}$. Therefore $\mathcal{S}$ and ℓ can be expressed as

$$\ell = 2\int_0^{z_*} \frac{1}{\sqrt{F(z)}}\frac{dz}{\sqrt{\frac{V^2(z)}{V^2(z_*)} - 1}}, \qquad \mathcal{S} = 2\int_\epsilon^{z_*} \frac{V(z)}{V(z_*)}\frac{M(z)dz}{\sqrt{\frac{V^2(z)}{V^2(z_*)} - 1}}, \tag{9}$$

where $V(z) = M(z)\sqrt{F(z)}$.

We are interested in studying the asymptotics of $\mathcal{S}$ at large ℓ. There are two options to have $\ell \to \infty$.

- The existence of a stationary point of $V(z)$, i.e. $V'|_{z=z_{DW}} = 0$, one calls this point as a dynamical wall (DW) point,

$$\frac{M'(z)}{M(z)} + \frac{1}{2}\frac{F'(z)}{F(z)}\Big|_{z=z_{DW}} = 0. \tag{10}$$

  In this case one takes the top point z_* equal to z_{DW} and since near the top point

$$\sqrt{\frac{V^2(z)}{V^2(z_{DW})} - 1}\Big|_{z\sim z_{DW}=z_*} = \sqrt{\frac{V''(z_{DW})}{V(z_{DW})}}(z - z_*) + O((z - z_*)^2), \tag{11}$$

  one gets

$$\ell \underset{z\to z_*}{\sim} \frac{1}{\sqrt{F(z_{DW})}}\sqrt{\frac{V(z_{DW})}{V''(z_{DW})}}\log(z - z_*), \qquad \mathcal{S} \underset{z\to z_*}{\sim} M(z_{DW})\sqrt{\frac{V(z_{DW})}{V''(z_{DW})}}\log(z - z_*).$$

  Hence $\mathcal{S} \sim M(z_{DW}) \cdot \sqrt{F(z_{DW})} \cdot \ell$ and $\sigma_{DW} = M(z_{DW})\ \sqrt{F(z_{DW})}$.

- There is no stationary point of $V(z)$ in the region $0 < z < z_h$ and we suppose that near horizon we have the behaviour $F(z) = \mathfrak{f} \cdot (z_h - z) + O((z_h - z)^2)$, i.e. near horizon the string stretches on the horizon. In this case we take $z_* = z_h$ and there are the following options:

  – if $M(z_h) \neq \infty$ we have $\ell \to \infty, \quad S \to 0$;
  – if $M(z) \underset{z\to z_h}{\to} \infty$, for example $M(z) \underset{z\sim z_h}{\sim} \frac{\mathfrak{m}(z_h)}{\sqrt{z-z_h}}$, we have

$$\ell \underset{z\to z_h}{\sim} \frac{1}{\sqrt{\mathfrak{f}(z_h)}}\frac{1}{\sqrt{-\frac{2V'(z_h)}{V(z_h)}}}\log(z - z_h), \quad \mathcal{S} \underset{z\to z_*}{\sim} \mathfrak{m}(z_h)\frac{1}{\sqrt{-\frac{2V'(z_h)}{V(z_h)}}}\log(z - z_h),$$

  and therefore, $\sigma_h = \mathfrak{m}(z_h)\,\mathfrak{f}^{1/2}(z_h)$.

3 Wilson loops, confinement and phase diagram

In [5] (see also [23]), we have studied the temporal Wilson loops, extended in longitudinal and transversal directions, by calculating the minimal surfaces of the corresponding probing open string world-sheet in anisotropic backgrounds with various temperatures and chemical potentials. We have found that DW locations depend on the orientation of the quark pairs, that gives a crossover transition line between confinement/deconfinement phases in the dual gauge theory. Instability of the background leads to the appearance of the critical points $(\mu_{\vartheta,b}, T_{\vartheta,b})$ depending on the orientation ϑ of quark-antiquark pairs in respect to the heavy ions collision line. The case of arbitrary orientation has been considered in [24], see also [25], where corresponding phase diagrams are presented.

4 Spatial Wilson loops and drag forces

As has been shown in [26, 27] the energy lost and drag forces can be calculated with the holography and moreover, the within the duality the low momenta drag coefficients for heavy quarks are proportional to the spatial string tension [28], see also [29]. The drag force is a characteristic of heavy quark moving through the plasma. Now let us discuss a string attached to an external quark that moves with speed v in the x direction. As has been noted in [28] the quark-antiquark $\bar{Q}Q$ configuration with large separation is the mirror reflected solution of single heavy probe. In [29] the drag coefficient is calculated from the momentum flow flowing from the boundary to the horizon along the string worldsheet, as originally described in [21] for AdS space. The main point concerning the spatial Wilson loops is that they always, even above T_c, obey an area law. We will see this explicitly in all considered below examples.

4.1 Spatial Wilson loops in the background (2)

In this section we consider behaviour of different oriented spatial Wilson loops in the background (2). We denote $\mathrm{WL}_{x_iX_j}$ the rectangular strip Wilson loop on the (x_ix_j) plane, $x_i = \{x, y_1, y_2\}$, with the assumption that this strip is infinite along the x_j-direction.

4.1.1 Spatial WL_{xY}

We start from WL_{xY} and parametrize the string world-sheet as $\sigma^1 = x$, $\sigma^2 = y_1$. Assuming the dependence $z = z(x)$ we get the Nambu-Goto action

$$\mathcal{S}_{xY} = \frac{T}{2\pi\alpha}\int_{-\ell}^{\ell} V_{x,eff}\sqrt{1+\frac{z'^2}{f}}, \quad V_{x,eff} = \frac{b_s}{z^{1+1/\nu}} = \frac{e^{P(z)+\sqrt{\frac{2}{3}}\phi(z)}}{z^{1+1/\nu}} \tag{12}$$

This is a particular case of (8), we add a subscription index for M, F and V to indicate what case we consider. $M_{xY} = \frac{b_s(z)}{z^{1+1/\nu}\sqrt{f(z)}}$, $F_{xY} = f$, and $V_{xY}(z) = \frac{b_s(z)}{z^{1+1/\nu}} = V_{x,eff}$. As has been explained in sect.2.2 there are two options to have $\ell \to \infty$:

- the existence a stationary point z_{DW} of $V_{xY}(z)$

$$LHS_{\,xY}(z, c, \nu) \equiv P'(z) + \sqrt{\frac{2}{3}}\phi'(z) - \frac{1+1/\nu}{z}\Big|_{z=z_{DW}} = 0, \tag{13}$$

  and then $\sigma_{xY,DW} = \frac{b_s(z_{DW})}{z_{DW}^{1+1/\nu}} = V_{x,eff}(z_{DW})$.

- we take $z_* = z_h$ and get $\sigma_{xY,z_h} = \frac{b_s(z_h)}{z_h^{1+1/\nu}} = V_{x,eff}(z_h)$.

We compare these two σ_{xY}, $\sigma_{xY,DW}$ and σ_{xY,z_h}, in Fig.2.

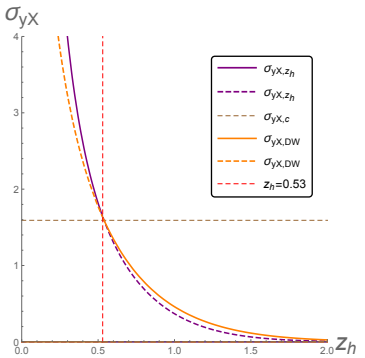

Figure 2: The dependence of the tension of the spatial Wilson loop W_{xY} (the same is for W_{yX}) on z_h.

4.2 Spatial WL_{yX}

The action for the rectangular strip infinite along the x-direction is

$$S_{yX} = \frac{T}{2\pi\alpha}\int_{-\ell}^{\ell}\frac{b_s(z)}{z^2}\sqrt{z^{2-2/\nu}+\frac{z'^2}{f}} \tag{14}$$

This is a particular case of (8) with $M_{yX} = \frac{b_s(z)}{z^2\sqrt{f}}$, $V_{yX}(z) = \frac{b_s(z)}{z^{1+1/\nu}}$ and $F_{yX} = f(z)z^{2-2/\nu}$. There are two options to have $\ell \to \infty$.

- There exists a stationary point z_{DW} of $V_{yX}(z)$

$$LHS_{yX}(z,c,\nu) \equiv P'(z) + \sqrt{\frac{2}{3}}\phi'(z) - \frac{\frac{1}{\nu}+1}{z}\Big|_{z=z_{DW,yX}} = 0 \tag{15}$$

  and $\sigma_{yX,DW} = \frac{b_s(z_{DW})}{z_{DW}^{1+1/\nu}} \equiv V_{yX}(z_{DW}) = V_{x,eff}(z_{DW})$.

- We take $z_* = z_h$ and get $\sigma_{yX,z_h} = \frac{b_s(z_h)}{z_h^{1+1/\nu}}$

We compare these two σ_{yX} in Fig.2. It is also interesting to see the dependence of different σ on T at different chemical potential, see Fig.3.

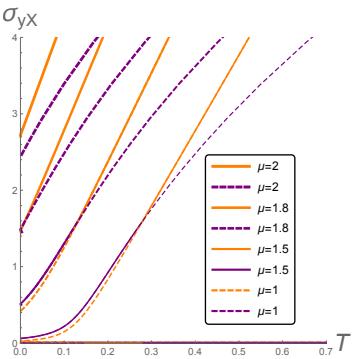

Figure 3: The dependence of the tension of the spatial Wilson loop W_{xY} (A) (the same for W_{yX}) on the temperature.

4.3 Spatial WL$_{yY}$

It is also interesting to consider WL$_{yY}$, here we denote y_1 as y and y_2 as Y. Choose for parametrization of the world-sheet as $\sigma^1 = y$, $\sigma^2 = Y$. Taking into account $z = z(y)$ one can write down the action for the rectangular strip in the transversal plane as

$$S_{yY} = \frac{Y}{2\pi\alpha}\int_{-\ell}^{\ell}\frac{b_s(z)}{z^{1+1/\nu}}\sqrt{z^{2-2/\nu} + \frac{z'^2}{f}}dy. \tag{16}$$

In this case we get the action (8) with $M_{yY} = \frac{b_s(z)}{z^{1+1/\nu}\sqrt{f}}$, $F_{yY} = fz^{2-2/\nu}$, $V_{yY} = \frac{b_s(z)}{z^{2/\nu}}$. In this case there are no solutions to the DW position equation

$$LHS_{yY}(z,c,\nu) \equiv P'(z) + \sqrt{\frac{2}{3}}\phi'(z) - \frac{\frac{2}{\nu}}{z}\Big|_{z=z_{DW,yY}} = 0, \tag{17}$$

for $c < 0$, see Fig.4 and we have $\sigma_{yY,z_h} = \frac{b(z_h)}{z_h^{2/\nu}}$.

To summarize the section, we have found that in the case of longitudinal-traversal mixed orientations there is the phase transition: at some points on (T,μ)-plane the temperature (or chemical potential) dependence of the string tension exhibits a jump of derivative.

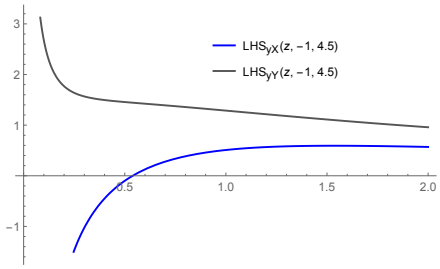

Figure 4: The dependence of *LHS* , defined in (13) (the same as (15)) and (17) for the spatial Wilson loop W_{xY}, W_{yX} and W_{yY}, on z.

5 Conclusion

To conclude, I would like to stress that holographic models are some kind of phenomenological models with few number of parameters. We have considered the anisotropic model of HIC that *describes*: multiplicity, quark confinement and *predicts*: crossover transition line between confinement/deconfinement phases anisotropy in hadron spectrum (for a short time after collisions) and phase transition for drag forces in the mixed longitude-transversal directions.

References

[1] I. Aref'eva, "Multiplicity and theremalization time in heavy-ions collisions", EPJ Web Conf. **125**, 01007 (2016)
[2] I. Aref'eva, Holography for Heavy Ions Collisions at LHC and NICA , EPJ Web Conf. **164**, 01014 (2017)
[3] I. Ya. Aref'eva, *Phys. Usp.* **57** (2014) 527
[4] M. Strickland, *Pramana* **84**, 671 (2015)
[5] I. Aref'eva and K. Rannu, JHEP **1805**, 206 (2018)
[6] Y. Yang and P.-H. Yuan, JHEP 1512 161 (2015)
[7] T. Azeyanagi, W. Li and T. Takayanagi, JHEP 0906 (2009) 084
[8] A. Donos, J. P. Gauntlett and C. Pantelidou JHEP 1201 (2012) 061
[9] I. Ya. Aref'eva, A. A. Golubtsova and E. Gourgoulhon, JHEP **1609**, 142 (2016)
[10] I. Ya. Aref 'eva, A. A. Golubtsova and G. Policastro, "Exact holographic RG flows and the $A_1 \times A_1$ Toda chain," arXiv:1803.06764 [hep-th]
[11] I. Ya. Arefeva, Phys. Lett. B **325**, 171 (1994)
[12] D. Giataganas, U. Gursoy and J. F. Pedraza, "Strongly-coupled anisotropic gauge theories and holography," arXiv:1708.05691 [hep-th]
[13] T. Azeyanagi, W. Li and T. Takayanagi, JHEP **0906**, 084 (2009)
[14] D. Mateos and D. Trancanelli, Phys. Rev. Lett. **107**, 101601 (2011)
[15] D. Mateos and D. Trancanelli, JHEP **1107**, 054 (2011)
[16] U. Gursoy and E. Kiritsis, JHEP 02, 032 (2008), arXiv:0707.1324 [hep-th].
[17] U. Gursoy, E. Kiritsis, and F. Nitti, JHEP 02, 019 (2008), arXiv:0707.1349 [hep-th].
[18] S. S. Gubser and A. Nellore, Phys. Rev. D78, 086007 (2008), arXiv:0804.0434 [hep-th].
[19] S. S. Gubser at al Phys. Rev. Lett. 101, 131601 (2008)
[20] I. Y. Arefeva, Phys. Lett. **93B**, 347 (1980)

[21] E. Witten, Adv.Theor.Math.Phys. 2, 505 (1998)
[22] D. S. Ageev et al, Nucl. Phys. B **931**, 506 (2018)
[23] K. Rannu, "Holographic anisotropic background with confinement-deconfinement phase transition", on the XXth International Seminar “Quarks-2018”.
[24] I. Aref’eva, K. Rannu and P. Slepov, “Orientation Dependence of Confinement-Deconfinement Phase Transition in Anisotropic Media,” arXiv:1808.05596 [hep-th].
[25] P. Slepov, “Orientation Dependence of Confinement-Deconfinement Phase Transition in Anisotropic Media”, on the XXth International Seminar “Quarks-2018”.
[26] C. P. Herzog et al, JHEP **0607**, 013 (2006)
[27] S. S. Gubser, Phys. Rev. D **74**, 126005 (2006)
[28] S. J. Sin and I. Zahed, Phys. Lett. B **648**, 318 (2007)
[29] O. Andreev, “Drag Force on Heavy Quarks and Spatial String Tension,” arXiv:1707.05045 [hep-ph]